Systematic Parameter Determination Aimed at a Catalyst-controlled Asymmetric Rh(I)-Catalyzed Pauson-Khand Reaction

Yifan Qi, Luke T. Jesikiewicz, Grace E. Scofield, Peng Liu* and Kay M. Brummond*

Department of Chemistry, University of Pittsburgh, Pittsburgh, Pennsylvania 15260, United States

Keywords: Catalyst-control, Asymmetric Pauson–Khand reaction, Chiral quaternary carbon centers, Solvent effect, Counterion effect, Bisphosphine ligand effect, Substrate effect, Descriptor selection

ABSTRACT: Transition metal-catalyzed carbocyclization reactions have revolutionized the synthesis of complex cyclic organic compounds. Yet, subtle substrate changes can significantly alter reaction pathways. The asymmetric Rh(I)-catalyzed Pauson-Khand reaction (PKR) exemplifies such a reaction, being hindered by a narrow substrate scope and competing reactivity modes. In this study, we identified parameters predictive of yield and enantioselectivity in the catalyst-controlled asymmetric PKR, using 1,6-enynes with a 2,2-disubstituted alkene. In this way, ring-fused cyclopentenones can be formed with chiral quaternary carbon centers. Using bisphosphine ligand parameters from palladium complexes, including HOMO energy and the angle formed by the phosphorous aryl groups on the ligand, we established strong correlations with experimental % *ee* (R^2=0.94 and 0.98) for two distinct precursors. Solvent dipole moments correlated with % *ee* for high dipole moment precursors (R^2=0.97), while Abraham's hydrogen bond basicity is more relevant for low dipole moment precursors (R^2=0.93). Additionally, counterions were found to have a significant impact on PKR reactivity and selectivity, as does the steric demand of the alkyne substituent of the enyne precursor. In the latter case, %*ee* correlates with Sterimol B_1 values for products with different alkyne substituents (R^2=0.96). Furthermore, the computed C≡C wavenumber of the enyne precursor can be directly aligned with the yield of the asymmetric PKR.

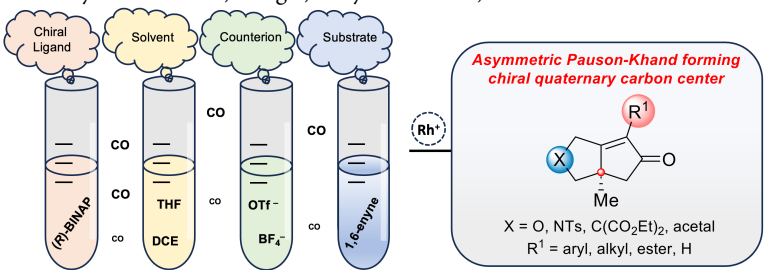

INTRODUCTION

The Pauson-Khand reaction (PKR) is a powerful method for synthesizing ring-fused cyclopentenones[1–4] – products equipped for building up complexity to provide compound structures in bioactive natural products and commercial drugs (Figure 1A).[5–11] Relying on the structural features of the substrate (*e.g.*, rigidity, sterics, and electronics), racemic PKRs have been utilized mid-synthetic sequence to provide good yields and high diastereoselectivities of key synthetic targets. However, the *asymmetric PKR* has the potential to generate chiral non-racemic 5,5-, 5,6-, and 5,7-ring systems directly without these limitations. Rh(I)-catalyzed PKRs offer the most versatile asymmetric PKR protocol to date, and yet, the substrate structure remains a critical hindrance to a generalized enantioselective PKR.

With the goal of realizing a fully catalyst-controlled asymmetric Rh(I)-catalyzed PKR, we and others have focused on gaining an understanding of the key elementary steps of this transformation. For example, using a combination of experiment and theory, we have identified that the oxidative cyclization step is stereo-determining and have utilized the corresponding transition state structures and activation barriers to inform our catalyst design. This approach has allowed us to extend the asymmetric PKR to allene-ynes.[12]

Despite these successes, reported studies have generally focused on the influence of only a single factor on the reactivity and selectivity of the PKR. For instance, Jeong showed that electron-withdrawing aryl groups on the bisphosphine ligand of the Rh(I) catalyst generally provided higher enantioselectivities (*ees*), albeit with variable yields and significant sensitivity to substrate structure (Figure 1B).[13]

Similarly, the role that counterion plays on PKR reactivity and selectivity has been evaluated but remains poorly understood. Pfaltz performed an extensive study on counterion effects using Ir-Phox catalysts and showed that the counterion had a strong influence on the PKR yield and *ees* of three different enynes. In these cases, small weakly coordinating counterions (OTf, SbF_6^-, and BF_4^-) gave higher yields and *ees*, compared to larger non-coordinating anions such as $BArF^-$. When –OTs, –OMs, and –TFA were used as counterions, only trace amounts of PKR products were observed (Figure 1C).[14] This is likely due to the electronic requirements of the reaction center, which differ between substrates. For example, the key mechanistic step when an electron withdrawing reaction center is present involves complexation of the enyne to the Rh(I) metal and reductive elimination, whereas the oxidative cyclization step dominates reaction outcome when the complex has a more electron-donating reaction center. The analysis is complicated further as the solvent

impacts the coordinating ability of the counterion. In less polar solvents the counterion is predicted to be closer to the reaction center, existing as a contact ion-pair with the catalyst. Conversely, in more polar solvents the counterion is isolated from the reaction center, leading to a dissociated ion-pair.[15]

In yet other efforts, computed Gibbs free energy values for the complexation of the enyne to **1**, **3a**, and **3b** show that the auxiliary ligand may greatly impact the catalyst equilibria (Figure 1D). For example, complexation of the non-sterically demanding ether-tethered enyne with a monosubstituted alkene to the Rh having two COs, **1**, is highly endergonic (ΔG= 27.6 kcal/mol) and slightly endergonic for **3a** (ΔG =0.8 kcal/mol) and exergonic for **3b** (ΔG = −6.8 kcal/mol).[16] Jeong *et al.* demonstrated that the asymmetric Rh(I)-catalyzed PKR gives higher *ees* in the presence of coordinating solvents like THF, and postulated that these solvents compete with CO as ligands for Rh(I). Solvent coordination shifts the enyne complexation equilibria towards the more reactive catalytic species **2** and **3**. On the other hand, non-coordinating solvents, such as toluene, promote formation of the less reactive CO saturated **1**; reactions in non-coordinating solvents required higher reaction temperatures (Figure 1D).[17]

Recently, DFT calculations have been used to establish the oxidative cyclization step as rate- and enantio-determining for the asymmetric PKR for an ether-tethered enyne with a monosubstituted alkene.[16] Initial rate studies showed that the auxiliary ligand on the Rh(I)-enyne complex is an important reactivity driver. When using the bidentate bisphosphine (*R*)-BINAP as a chiral ligand, the PKR was 21,400-fold faster than when using CO-only conditions (Figure 1E). The monodentate phosphoramidite ligand (*S*)-Monophos showed an intermediate level of reactivity. Another important finding included two distinct reaction pathways that produced enantiomeric PKR products. The TSs for the 4-coordinated pathway are favored over the 5-coordinated by 3.5 kcal/mol under low CO concentration (Figure 1E).[16]

While these studies have contributed greatly to our understanding of the asymmetric Rh(I)-catalyzed PKR mechanism, it has done more to reveal the complex interrelated factors that control PKR selectivity and reactivity (e.g., CO concentration, ligand identity, solvent, and substrate structure) than to produce significant advances in asymmetric PKR reaction scope. If anything, the growing appreciation of the mechanistic complexity of the asymmetric PKR has hindered its application to complex molecular target synthesis.

Given that these studies have evaluated reaction parameters largely in isolation, it remains difficult to discern their interrelationships. As such, catalyst and PKR conditions optimization have largely been arbitrary and empirical. To address this gap in asymmetric PKR methodology, we set out to combine previous experimental and computational mechanistic insight (Figures 1B–1E) with a systematic evaluation of a variety of reaction conditions to correlate product yield and enantioselectivity with parameters for an array of enyne precursors (Figure 1F). Our initial studies utilized the synthetically useful but challenging 1,6-enyne precursors possessing a 2,2-disubstituted alkene for which there is little data (Figure 1F). (Prior to 2023 only two enynes featuring a 2,2-disubstituted alkene were successfully shown to undergo an asymmetric Ir(I) or Rh(I) *catalyst-controlled* PKR.[14,18–25] In 2023, Baik and Evans *et. al.* showed that an asymmetric PKR using 2,2-disubstituted alkenes could be effected so long as the enyne precursors bore a chloroacetylene group.[26]) Upon PKR, these substrates provide chiral non-racemic 5,5-ring systems having a quaternary (4°) carbon at the ring fusion.[27–29] Despite their value, these precursors are also prone to undergoing reactions other than the PKR.[30–33]

Herein, we report parameters for the chiral ligand, [13,16,26] solvent,[17,34–36] and substrate that show excellent correlation with product % *ee* (Figure 1F). We also identified qualitative descriptors for the substrate and the Rh precatalyst counterion that are predictive of reactivity trends and yield (Figure 1F). Efforts to identify parameters predictive of % *ee* and yield, led to thirteen novel chiral non-racemic 5,5-ring systems bearing a 4° carbon.

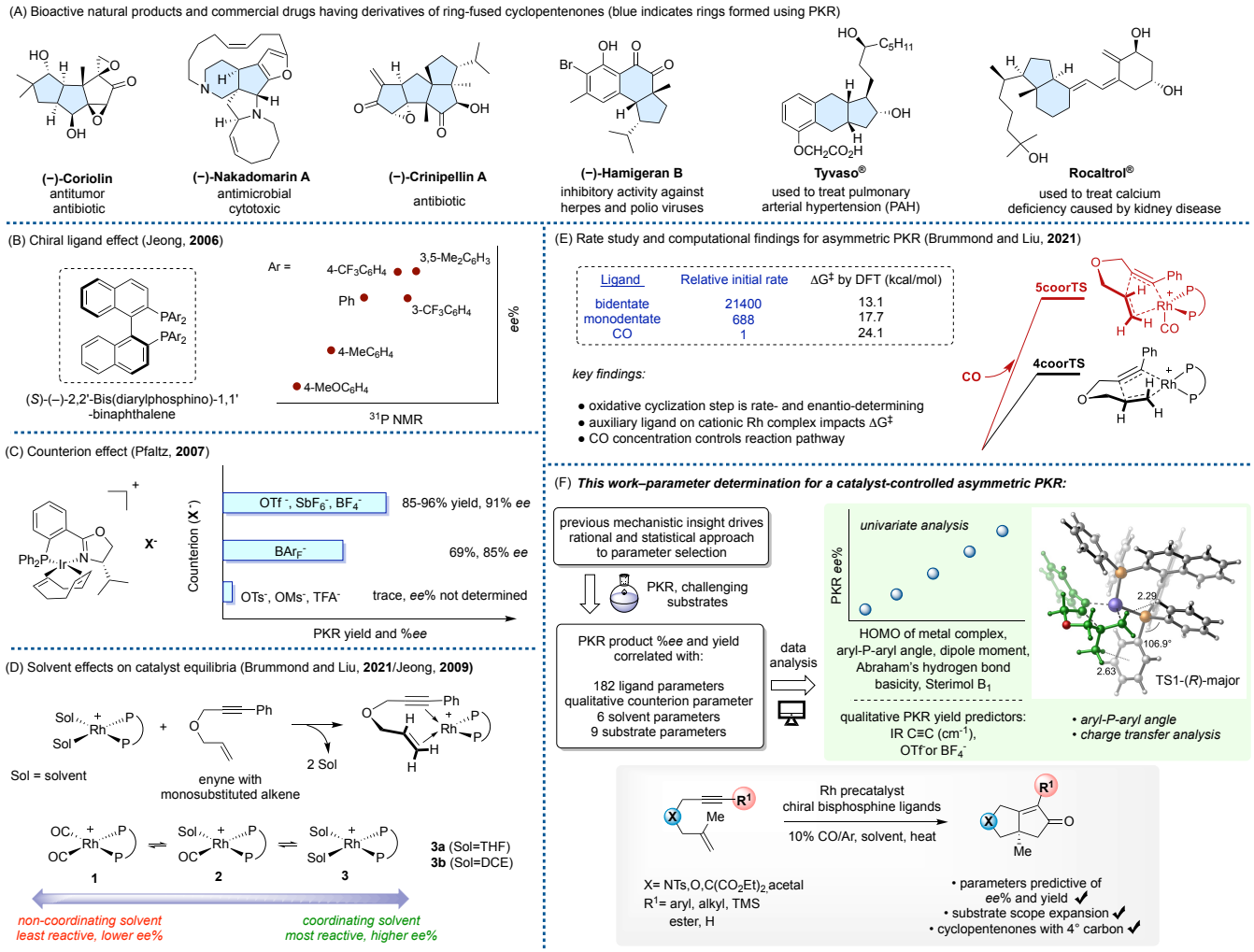

Figure 1. (A) Bioactive natural products and representative drugs accessed through Pauson-Khand reactions; (B) Impact of electronic character of bisphosphine ligands on PKR % *ee*; (C) Impact of counterions on PKR reactivity and selectivity; (D) Previous independent studies by Brummond/Liu and Jeong showing the impact of ancillary ligands on enyne binding and catalyst equilibria; (E)Previous rate study and computational findings for asymmetric PKR ; (F) This work.

RESULTS AND DISCUSSION

Identifying chiral bisphosphine ligand descriptors for Rh(I)-catalyzed PKR yield and enantioselectivity. To identify potential chiral ligand parameters that correlate with PKR yield and enantioselectivity, five bisphosphine ligands were evaluated including a combination of a binaphthyl or biphenyl backbone and either tolyl, mesityl, and 3,5-di-tert-butyl-4-methoxy aryl groups on the donor phosphine atoms (e.g., (*R*)-BINAP (**L1**), (*R*)-Tol-BINAP (**L2**), (*R*)-DM-BINAP (**L3**), (*R*)-DM-SEGPHOS (**L4**), (*R*)-DTBM-SEGPHOS (**L5**)). These relatively electron-rich bisphosphines were selected in order to take advantage of their predicted favorable Gibbs free energy barrier for oxidative cyclization.[16] In the event, $Rh(cod)_2OTf$ precatalyst was reacted with each ligand in the presence of enyne **4a** or **6a**, in either THF or DCE under a 10% concentration of CO in argon. The overall efficiency and selectivity of each ligand was determined by ^1H NMR and chiral HPLC of the crude reaction mixture. $Rh(cod)_2OTf$ was chosen as the Rh(I) source for these reactions as it afforded the PKR products in the highest yields and % *ee* for nearly all substrates (see Table 4 below), with the exception of the all-carbon tethered precursors **8b** and **10a**. The concentration of CO was chosen to maximize the enantioselectivity of the PKR products.[16] Both –NTs and ether-tethered precursors were utilized in the ligand study given their distinct calculated dipole moments (5.47 and 1.1 Debye, respectively ωB97X-V 6-311+G(2df,2p)//ωB97X-D 6-311+) and their difference in size.

Reaction of enyne **4a** in the presence of ligands **L1**, **L2**, **L3**, and **L4**, provided product **5a** in high yields (96–99%) and good to excellent enantioselectivity (70-90% *ee*), with reaction times varying from 19–27 h (Table 1, entries 1–4). Utilizing ligand **L5**, the PKR of enyne **4a** was more sluggish, affording only 39% yield of compound **5a** and 56% recovered starting material after 40 h. In this latter case, steric repulsion between the tert-butyl groups of the chiral ligand and the enyne could be responsible for the low reaction efficiency based on the computed oxidative cyclization TS structures (Figure 3).

Table 1. Evaluation of ligands in the asymmetric PKR of precursors **4a** and **6a**

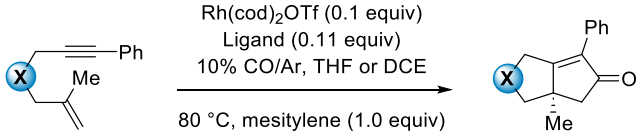

4a, X=NTs
6a, X=O

5a, X=NTs
7a, X=O

A systematic examination of a small ligand library:

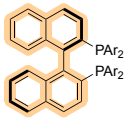

· Ar = Ph, (*R*)-BINAP, **L1**
· Ar = 4-methyl-C_6H_4, (*R*)-Tol-BINAP, **L2**
· Ar = 3,5-dimethyl-C_6H_3, (*R*)-DM-BINAP, **L3**

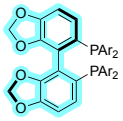

· Ar = 3,5-dimethyl-C_6H_3, (*R*)-DM-SEGPHOS, **L4**
· Ar = 3,5-di-tert-butyl-4-OMe-C_6H_2 (*R*)-DTBM-SEGPHOS, **L5**

entry	ligand	time (h)	yield[a] (%)	*er*[b] (% *ee*)
X=NTs (**4a**), in THF				**5a**
1	**L1**	22	99	95:5 (90)
2	**L2**	21	96	91:9 (82)
3	**L3**	19	96	89:11 (78)
4	**L4**	27	98	85:15 (70)
5	**L5**	40	39(56)[c]	93:7 (86)
X= O (**6a**), in DCE				**7a**
6[d]	**L1**	23	84	94:6 (89)
7	**L2**	29	79(5)[c]	83:17 (66)
8	**L3**	20	74	70:30 (40)
9	**L4**	17	62	74:26 (47)
10	**L5**	44	69(24)[c]	89:11 (78)

[a]yield determined by ^{1}H NMR of the crude reaction by comparison to an internal standard (mesitylene, s, 6.78 ppm) to the product peak (d, 4.62 ppm of **5a**; d, 4.61 ppm of **7a**); [b]*ee*s determined by HPLC; [c]number in parentheses represents the yield of recovered starting material, as determined by ^{1}H NMR of crude material; [d]reaction performed at 85 °C.

In the conversion of ether-containing precursor **6a**, ligands **L1**–**L4** gave moderate yields of bicyclic compound **7a** (62–84%) with a broader range of selectivity observed (40–89% *ee*) (Table 1, entries 6–9). Ligand **L5** still resulted in a slower reaction, now providing 69% yield of product **7a** and 24% recovered starting material after 44 h (entry 10).

To identify parameters that are predictive of this experimentally observed enantioselectivity, we correlated the ln(*ee*) observed for reaction of enyne **4a** with each of the ligands to 181 computed descriptors for bisphosphine ligands complexed to Pd(II)Cl_2.[37] Although the computed TS structures of the Rh(I) bisphosphine enyne complex during the oxidative cyclization step show a twisted tetrahedral geometry, compared to the descriptor data representing a computed ground state, square planar $PdCl_2$/bisphosphine complex, these ligand parameters were successfully applied to a linear-regression modeling of the Rh(I)-catalyzed hydroformylation reaction.[37] The data was processed using MATLAB® with the threshold set to R^2=0.8. (see Supporting Information, Figure S35).

For the –NTs tethered precursor **4a**, six parameters met this threshold with HOMO energy of the Pd/ligand complexes showing the strongest correlation (R^2=0.94, Figure 2A and Figure S36 in SI). The findings for ligand **L5** further support the observed electronic influence on PKR *ee*; developing steric repulsions greatly decrease the rate of the PKR, but have no impact on the observed enantioselectivity (entry 5).

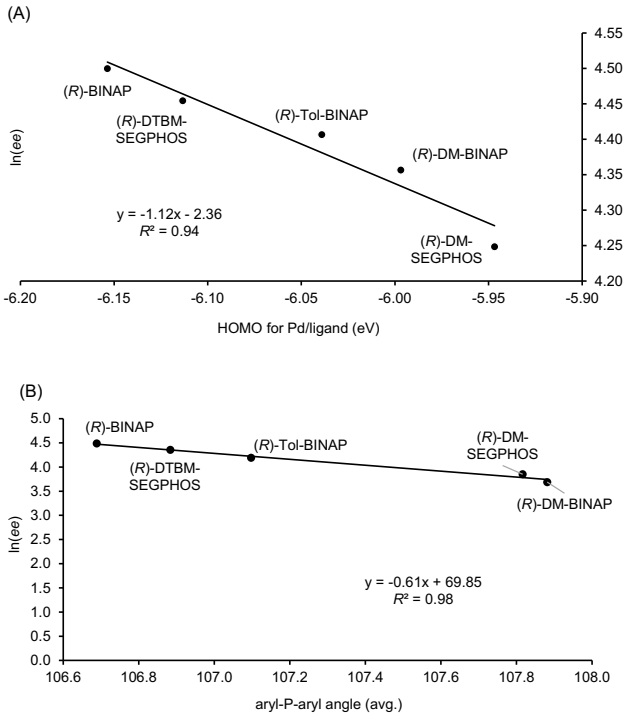

Figure 2. Correlation of ln(*ee*) with the best-performing parameter. (**A**) ln(*ee*) of **5a** with HOMO energy (highest occupied (Kohn-Sham) molecular orbital) for the Pd/ligand complex**.** (**B**) ln(*ee*) of **7a** with average aryl-P-aryl angle of the bisphosphine ligand.

A similar set of seven parameters showed good correlations with ln(*ee*) of ether **7a** (see Figure S38 in SI). In this case, the aryl-P-aryl angle (average) descriptor afforded the best correlation, featuring an R^2= 0.98 (Figure 2B). The HOMO energy descriptor for the Pd ligand complex gave a moderate correlation (R^2=0.83, see Figure S40 in SI).

That the preferred descriptors change between substrate classes is likely related to the varying interactions between the electronic and steric properties of the ligands and substrates. For electron-poor *N*-tosylated enynes, such as compound **4a**, the enantioselectivity is more sensitive to the electronic properties of the ligand. In contrast, for less electron-poor substrates such as ether **6a**, the steric nature of the ligand exerts more influence on the diastereomeric transition states, resulting in less consistent enantioselectivity being observed.[38]

To further understand these observations, we performed DFT calculations of the enantio-determining oxidative cyclization of ether **6a** with the (*R*)-BINAP (**L1**) and (*R*)-DM-BINAP (**L3**) ligands, as they produced the most significant difference in % *ee* in product **7a** (89 % vs. 40 % *ee*, respectively).[39] With the (*R*)-BINAP-supported Rh catalyst, the oxidative cyclization TS leading to the (*R*) product (**TS1-R**) is favored over the TS leading to the minor (*S*) product (**TS1-S**) by 4.1 kcal/mol (Figure 3A). Similar to previous studies,[16] the selectivity between π faces of the alkene directly impacts the steric interactions of the terminal alkene hydrogens with the chiral ligand. In **TS1-S**, the shorter H···H distance between a terminal alkenyl hydrogen and a hydrogen atom on the *P*-Ph group on the

ligand (2.19 Å), relative to **TS1-R** (2.29 Å), causes more substrate distortion[40] ($\Delta E_{dist\text{-}sub}$ = 53.0 vs. 50.4 kcal/mol). Additionally, **TS1-R** is stabilized through a C–H/π interaction between the alkene methyl hydrogens and one of the (*R*)-BINAP (**L1**) phenyl groups (2.63 Å, Figure 3A). This additional stabilization is reflected in a lower substrate–catalyst interaction energy (ΔE_{int}) in **TS1-R** relative to **TS1-S** (−32.6 vs. −29.0 kcal/mol).

The computed transition states with (*R*)-DM-BINAP (**L3**) share many of the structural features of those with (*R*)-BINAP (**L1**) (Figure 3B). For example, **TS2-S** is 3.5 kcal/mol less stable than **TS2-R** due to the steric clash between the terminal alkene hydrogens and the chiral ligand (2.21 vs. 2.23 Å in **TS2-R**), leading to an increase in substrate distortion (52.3 vs. 49.9 kcal/mol in **TS2-R**). (*R*)-DM-BINAP also experiences a stabilizing C–H/π interaction between the alkene methyl group and the phosphine aryl group in **TS2-R** (2.65 Å), leading to a lower ΔE_{int} (−31.4 vs. −28.8 kcal/mol).

Although the computed enantioselectivity ($\Delta\Delta G^{\ddagger}$) is higher than experimental observations with both ligands, an overestimation also observed in previous computational studies,[16] computations predicted the reaction with (*R*)-DM-BINAP is less enantioselective than that with (*R*)-BINAP ($\Delta\Delta G^{\ddagger}$ = 4.1 and 3.5 kcal/mol), which is consistent with the experimental ligand effect trend. The enantioselectivity difference could be attributed to both steric and electronic effects. Sterically, the larger aryl-P-aryl angle between the two *P*-aryl groups on (*R*)-DM-BINAP (107.7° in **TS2-R** vs. 106.9° in **TS1-R**) effectively positions the P-aryl groups further away from the terminal alkenyl group on the substrate, minimizing ligand–substrate steric repulsions, as evidenced by the longer H···H distance in **TS2-S** relative to **TS1-S** (2.21 Å vs. 2.19 Å). This explains the somewhat surprising observation that the ligand aryl-P-aryl angle descriptor correlates the best with the ln(*ee*) of the reaction (Figure 2B). Electronically, both TSs leading to the minor enantiomer (**TS1-S** and **TS2-S**) experience a higher degree of metal-to-substrate charge transfer, relative to the major TSs. Therefore, stronger donor ligands, like (*R*)-DM-BINAP, are expected to better stabilize the minor TS leading to a decrease in % *ee* than more electron-rich ligands. This further demonstrates why electronic descriptors, such as the HOMO energy of the Pd/ligand complex, also correlate well with the experimentally observed ln(*ee*).

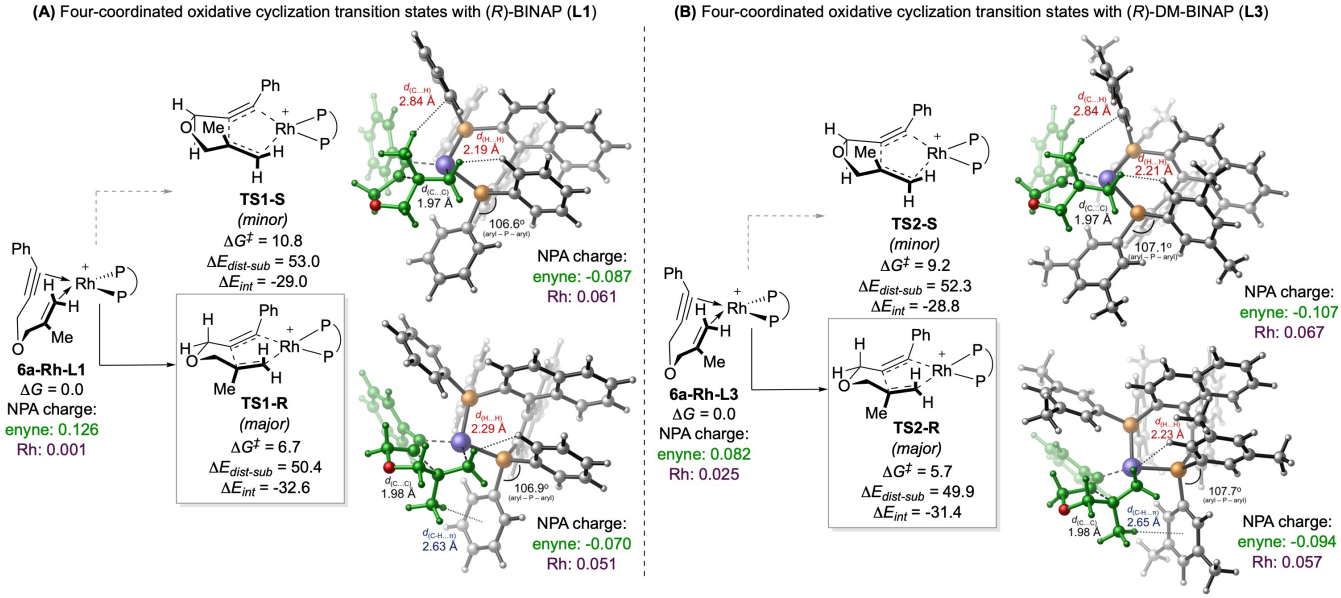

Figure 3. Lowest-energy transition state structures of oxidative cyclization of enyne **6a** with (*R*)-BINAP (**L1**) and (*R*)-DM-BINAP (**L3**) ligands. All energies are in kcal/mol.

The absolute configuration of (*R*)-**5ax**, using single crystal X-ray crystallography, provides further support for our computational predictions (Figure 4). Ketone **5a** (93:7 *er*) was initially converted to the hydrazone (*R*)-**5ax** using *p*-toluenesulfonyl hydrazine under acidic condition (see SI). Slow vapor diffusion of methanol into deuterated chloroform provided an X-ray quality crystal of **5ax**, from which X-ray analysis confirmed that the bridgehead carbon bears the (*R*) configuration, matching the major enantiomer predicted by DFT.

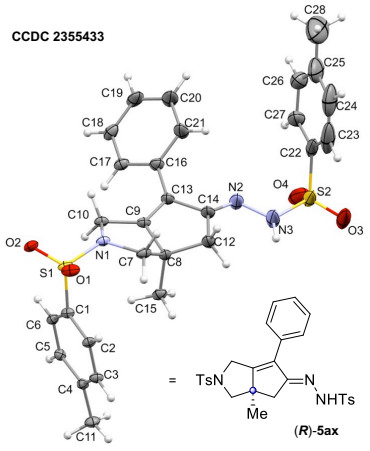

Figure 4. Single-crystal X-ray structure of hydrazone (*R*)-**5ax**

Identification of solvent parameters correlating with PKR yield and enantioselectivity. Our solvent study was guided by previous mechanistic work. We focused on solvents that had been successfully used previously in the Rh(I)-catalyzed PKR and that offered a range of coordinating abilities, based upon dipole moment (see Table S3 in SI). Eleven different solvents with dipole moments ranging from 0–2.86 were selected: tetrahydrofuran (THF), 1,2-dichloroethane (DCE), chloroform, chlorobenzene, trifluorotoluene, ethyl acetate, toluene, ethanol, 1,4-dioxane, trifluoroethanol, and dimethyl carbonate. These solvents also showed a range of Abraham's hydrogen bond basicity values (0.02–0.64), another measure of coordinating ability,[41] and a range of dielectric constants (2.219–27.68). Solvents previously used in PKRs—dibutyl ether, xylenes, and acetone—were not included due to technical difficulties associated with high and low boiling points.

–NTs and ether-tethered precursors **4a** and **6a** were evaluated, given the differences in yield and side product formation observed in an initial solvent study using $Rh(cod)_2BF_4$ (see Table S2 in SI). Ether-tethered **6a** is a model substrate for the asymmetric PKR, [18,20,24] whereas the asymmetric PKR of enyne **4a** had not yet been realized prior to this work. Enyne **4a** was reacted under PKR conditions with each solvent twice and the average yield and % *ee* of product **5a** were used for correlations. Enyne **6a** was only reacted with each solvent once. Each reaction was conducted with $Rh(cod)_2OTf$ (10 mol%), (*R*)-BINAP (11 mol%), 10% CO atmosphere/argon, 80 °C, solvent (0.05 M), and mesitylene (1.0 equiv) as an internal standard. An initial timepoint measurement was taken by ^1H NMR to establish the concentration of enyne **4a** (s, 4.25 ppm) or **6a** (s, 4.36 ppm), relative to the mesitylene (s, 6.78 ppm). A second measurement was taken at 24 h to determine: overall product yield (d, 4.62 ppm for **5a** and d, 4.61 ppm for **7a**), yield based on recovered starting material (b.r.s.m), and % *ee* (purified by prep TLC to get % *ee* by HPLC) (see Tables S4-S5 in SI).

The results for the –NTs tethered precursor **4a** are reported in Table 2. Solvent dipole moments and dielectric constants were plotted against yields, b.r.s.m., and % *ee* (see Figure S11-S16 in SI). In doing so, the solvents with the highest dipole moment were observed to afford the highest selectivity.

Table 2. Solvent study performed on enyne precursor **4a** using $Rh(cod)_2OTf$

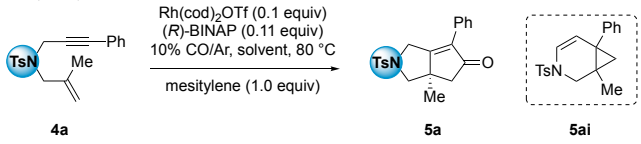

entry	solvent	yield[a] (**5ai**)[b] %	b.r.sm	%*ee*[a,c] **5a**
1	THF	99	99	90
2	1,2-dichloro-ethane	77 (6)	93	86
3	ethyl acetate	23 (trace)	94	88
4	trifluorotoluene	46 (trace)	82	82
5	trifluoroethanol	25 (4)	72	89
6	toluene	28 (5)	66	78
7	ethanol	35	71	89
8	chlorobenzene	32 (2)	73	66
9	1,4-dioxane	31 (2)	77	76
10	chloroform	65	89	94
11	dimethyl carbonate	48 (2)	90	83

[a]average of two experiments; determined by comparison of an internal standard (mesitylene: s, 6.78 ppm) to the product peak (d, 4.62 ppm) by ^1H NMR of crude material; [b]cycloisomerization side product yield; [c]*ee* determined by HPLC

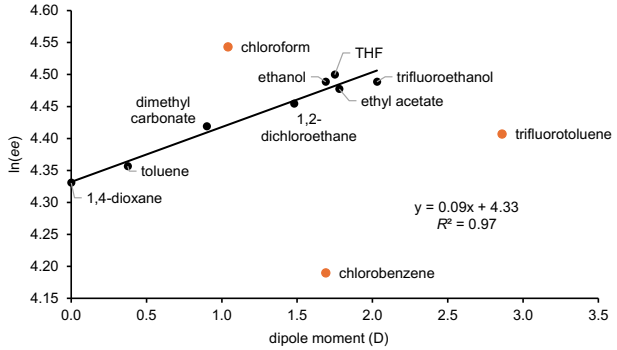

Figure 5. Correlation of ln(*ee*) of product **5a** with solvent dipole moments (D). Outliers are indicated with red dots.

Dipole moment showed a positive linear correlation with ln(*ee*) of product **5a** having an $R^2 = 0.97$ for eight of the eleven solvents (Figure 5). The outlier solvents include trifluorotoluene, chlorobenzene, and chloroform. For the aromatic solvents, arene complexes of the cationic Rh may be occurring, altering the energy difference between the diastereomeric oxidative cyclization TSs. Similarly with the lowest boiling point of the set, PKRs in chloroform occur at lower temperature (61.2 °C) than other solvents (all other reactions were heated to 80 °C), resulting in a higher kinetic selectivity.[42] Regarding chlorobenzene, analysis of experimental solvent π* and Taft β values, in relation to PKR % *ee*, revealed a cluster of solvents associated with low enantioselectivity (1,4-dioxane, toluene, chlorobenzene) (see Figure S20 in SI).

By comparison, ether **6a** reacted to give product **7a** in higher selectivity in halogenated solvents, with DCE and trifluorotoluene affording the highest enantioselectivity (87–89% *ee*) (Table 3). Conversely, THF, dimethyl carbonate, ethyl acetate, dioxane, and ethanol gave lower selectivity.

Table 3. Solvent study performed on enyne precursor **6a** using $Rh(cod)_2OTf$

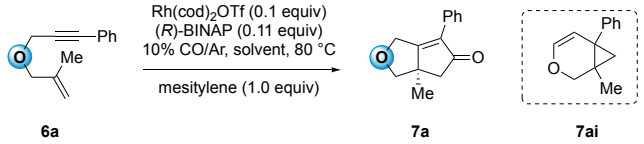

6a **7a** **7ai**

entry	solvent	yield[a] (**7ai**)[b] %	b.r.s.m	% *ee*[c] **7a**
1	THF	52	78	69
2	1,2-dichloro-ethane[d]	84 (13)	85	89
3	ethyl acetate	40	53	69
4	trifluorotoluene	26 (15)	55	87
5	trifluoroethanol	80	81	85
6	toluene	0 (4)	0	N/A
7	ethanol	52	53	69
8	chlorobenzene	22 (3)	67	84
9	1,4-dioxane	19 (4)	36	59
10	chloroform	trace	0	N/A
11	dimethyl carbonate	32	39	56

[a]yield determined by comparison of an internal standard (mesitylene: s, 6.78 ppm) to the product peak (d, 4.61 ppm) by ^{1}H NMR of crude material; [b]cycloisomerized side product yield; [c]*ee* determined by HPLC; [d]reaction performed at 85 °C.

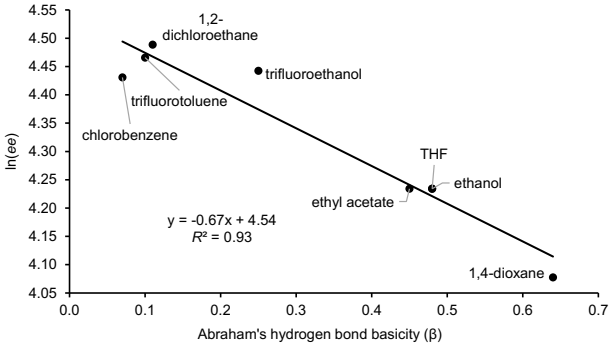

Figure 6. Correlation of ln(*ee*) of ether product **7a** with Abraham's hydrogen bond basicity of the solvents.

Abraham's hydrogen bond basicity (β), a solvent parameter that describes the ability of a solvent to act as a hydrogen bond acceptor,[43] shows a positive correlation with PKR ln(*ee*) of ether product **7a** for 8 of 11 solvents tested ($R^2 = 0.93$) (Figure 6). Toluene and chloroform were not included in the regression analysis as no PKR product was afforded after 24 h. Dimethyl carbonate was also excluded, as no β value was identified. Solvent π* values, another measure of solvent polarity, was plotted against ln(*ee*) of product **7a** and found to exhibit a moderate correlation ($R^2 = 0.85$) for 7 of the 11 solvents (π* was not identified for trifluorotoluene and dimethyl carbonate , see Table S3 and Figure S32 in SI).

This study shows that solvents strongly influence PKR outcomes (e.g., %ee and yield), and to a lesser extent, side-product formation. We attribute the variable solvent effectiveness for these two substrate classes to favorable electrostatic interactions between the enyne (D = 5.47 for **4a** and 1.1 for **6a**) and the solvent in the oxidative cyclization step. While this data supports that a single solvent parameter can be used to predict enantioselectivity for a distinct PKR substrate, the multifaceted nature of the PKR as indicated by the solvent outliers and the substrate dependency on solvent selection supports future studies directed towards using multivariate regression models (MLRs) for the selection of parameters.

***Identifying counterion descriptors that correlate to Rh(I)-catalyzed PKR yield and* enantioselectivity.** We then briefly examined the effect of three different Rh(I) precatalysts (e.g., $Rh(cod)_2BF_4$,[12,44] $Rh(cod)_2SbF_6$,[16] and $Rh(cod)_2OTf$[45]) to determine their impact on enantioselectivity and yield for six enyne precursors featuring different tethers and alkyne substituents. These pre-catalysts have been successfully used in the asymmetric PKR previously and differ only in their counterion, which is known to be a key factor in controlling PKR catalyst efficiency.[14] In all cases, (*R*)-BINAP was used as the chiral ligand, as it afforded the highest % *ee* of the five bisphosphine ligands examined above. The reactions were performed using a 10% CO/argon atmosphere with mesitylene as an internal standard, and the reaction temperature (60–100 °C) was selected based upon reaction rate. The solvent used for these reactions was informed by our solvent study. All reactions were allowed to go to completion or stopped when there was no visible progress.

Table 4. Counterion effect on selected enyne precursors featuring different tether and alkyne substituents

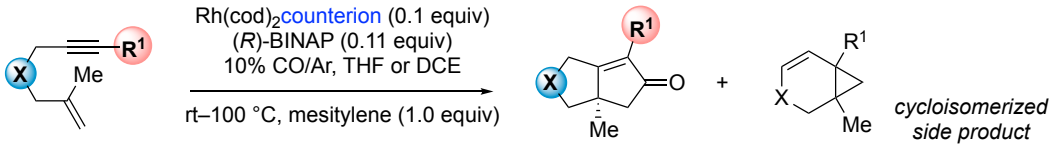

4a-**4b**, **6a**-**6b**, **8b**, **10a** **5a**-**5b**, **7a**-**7b**, **9b**, **11a** **5ai**-**5bi**, **7ai**-**7bi** **9bi**, **11ai**

entry	X	R^1	counterion	solvent	time (h)	temp. (°C)	PKR yield (SM remained)	cycloisomerized product yield (%)	PKR % *ee*
1	**4a**, NTs	Ph	BF_4^-	THF	28	80	**5a**, 91 (3)	**5ai**, 0	80
2	**4a**, NTs	Ph	SbF_6^-	THF	36	80	**5a**, 91 (2)	**5ai**, 0	77

3	**4a**, NTs	Ph	OTf^-	THF	22	80	**5a**, 99 (0)	**5ai**, 0	90
4	**4a**, NTs	Ph	BF_4^-	DCE	43	80	**5a**, 63(13)	**5ai**,7	89
5	**4a**, NTs	Ph	OTf-	DCE	46	80	**5a**, 68 (14)	**5ai**,17	86
6	**4b**, NTs	Me	BF_4^-	THF	28	60	**5b**, 44 (20)	**5bi**, 0	95
7	**4b**, NTs	Me	OTf^-	THF	20	60	**5b**, 71 (17)	**5bi**, 0	94
8	**6a**, O	Ph	BF_4^-	DCE	40	85	**7a**, 54 (0)	**7ai**, 31	90
9	**6a**, O	Ph	SbF_6^-	DCE	19	85	**7a**, 85 (trace)	**7ai**, 6	81
10	**6a**, O	Ph	OTf^-	DCE	23	85	**7a**, 84 (1)	**7ai**, 13	89
11	**6a**, O	Ph	BF4-	THF	45	80	**7a**, 8 (0)	**7ai**, 0	48
12	**6a**, O	Ph	OTf	THF	24	80	**7a**, 52 (33)	**7ai**, 0	69
13	**6b**, O	Me	BF_4^-	DCE	38	80	**7b**, 35 (0)	**7bi**, 55	75
14	**6b**, O	Me	OTf^-	DCE	27	80	**7b**, 66 (trace)	**7bi**, 25	75
15	**8b**, $(CO_2Et)_2$	Me	BF_4^-	DCE	15	95	**9b**, 93 (trace)	**9bi**, 0	55
16	**8b**, $C(CO_2Et)_2$	Me	OTf^-	DCE	11	95	**9b**, 67 (trace)	**9bi**, 0	46
17	**10a**, $C(CH_2O)_2CMe_2$	Ph	BF_4^-	DCE	88	100	**11a**, 81 (trace)	**11ai**, 0	43
18	**10a**, $C(CH_2O)_2CMe_2$	Ph	OTf^-	DCE	27	100	**11a**, 34 (2)	**11ai**, 0	76

Our experiments show that the counterion has a strong influence on the yield and % *ee* of the product. Further, a complex relationship exists between the counterion, the solvent, and the enyne precursor. For example, upon reaction of precursor **4a** (X= NTs, R^1=Ph) in THF, >90% yield was achieved without the formation of by-product **5ai**, regardless of catalyst counterion (Table 4, entries 1–3). Yet, the enantioselectivity varies from 77–90% *ee*. Conversely, when precursor **4a** (X= NTs, R^1=Ph) was reacted in DCE, the cycloisomerized product **5ai** is observed, albeit in small quantities (entries 4–5). For precursor **4b** (X= NTs, R^1=Me), both OTf^- and BF_4^- gave products of ~94% *ee*, but the yields were lower (71% and 44%), due to the reaction not going to completion (entries 6–7). The reaction of ether **6a** (X=O, R^1=Ph) was more sensitive to catalyst counterion, giving >84% yield for OTf^- and SbF_6^-, but only 54% yield for BF_4^- (entries 8–10). Regardless of counterion, reactions of ether **6a** resulted in the formation of cycloisomerization product **7ai**. The selectivities for product **7a** were constantly 81–90% *ee*, with the BF_4^- counterion giving the highest *ee*. When performing the reaction in THF, instead of DCE, the reaction is sluggish, giving either low yield or no reaction (entries 11–12). 75% ee was observed upon reaction of ether **6b** (X=O, R^1=Me) with both OTf^- and BF^-, while the yields varied (66% and 35%, respectively), relative to how much of by-product **7bi** was formed (entries 13–14). Reaction of the all-carbon analogue **8b** (X=$C(CO_2Et)_2$, R^1=Me) provided 93% yield with the BF_4^- counterion and 67% yield for OTF^-; however, both proceeded in low selectivity (46–55% *ee*). Similarly, acetal **10a** (R^1=Ph) gives 81% yield with BF_4^- and 34% yield for OTf in low to moderate selectivity (43–76% *ee*) (entries 17–18).

In general, higher yields and enantioselectivities were observed for enyne precursors featuring –NTs (**4a**, **4b**) and ether tethers (**6a**, **6b**) when using $Rh(cod)_2OTf$. However, for the malonate (**8b**) and acetal (**10a**) tethers, $Rh(cod)_2BF_4$ gave considerably higher yields, albeit in lower selectivity (43–76%*ee*). Reactions employing Rh(cod)2SbF_6 gave similar yields to $Rh(cod)_2OTf$, but in somewhat lower selectivity (entries 2 and 9).

For all enynes, PKR was faster when using $Rh(cod)_2OTf$. Consiglio and Schmid have shown that the degree of ion-pairing for [Rh(1,5-cod)Biphemp]counteranion, where counteranion = BF_4^-, PF_6^-, OTf^-, is inversely correlated with catalytic activity for the asymmetric PKR. For example, they showed that using [Rh(1,5-cod)Biphemp]OTf, which has the lowest ion-pairing, has the highest catalytic activity.[46] Our findings, using six different enynes and two solvents, show that this is a general principle of the asymmetric PKR.

The strong influence that the counterion has on yield is dependent upon the substrate and solvent. For example, when using DCE, we observed lower yields for ether tethers (entries 8–10, 13-14) which can be attributed to the formation of bicyclo[4.1.0]heptane side-products **7ai** and **7bi** in 6–55% yield. We only observe the formation of this side-product in the more polar solvent, DCE (ε =10.42), which favors a dissociated ion-pair and a more electron deficient Rh(I)-alkyne complex, relative to the complex in a less polar solvent THF (ε =7.52). This leads to a reaction energy profile that favors a [1,2]-hydrogen shift (**II**→**III**, see Figure S49 in SI) promoted cycloisomerization reaction over the oxidative cyclization of the PKR (**IV**→**V**, see Figure S47 in SI). The all-carbon tethers are an exception to this trend, as the [1,2]-hydrogen shift is inaccessible. Others have shown that formation of cycloisomerization side-products requires a heteroatom in the tether when using Pt or Au catalysis.[47]

Identification of substrate descriptors correlating with PKR yield and enantioselectivity. To determine the effects of substrate structure on the asymmetric Rh(I)-catalyzed PKR, enynes containing different tethers (X = NTs, O, $C(CO_2Et)$, and acetal), and alkyne substituents (R^1 = Ph, aryl, CO_2Me, Me, H, TMS) were evaluated. The enyne alkenyl group was held constant. The PKR conditions used for each substrate were based upon our findings in the chiral ligand, solvent, and counterion studies reported above. The PKR products afforded, in addition to reaction yields, % *ee*, reaction time, and side-products, for a range of heteroatom and carbon-tethered 1,6-enynes with 2,2-disubstituted alkenes are depicted in Scheme 1.

Our experiments show that the alkynyl substituent had the strongest influence on the PKR yield and reactivity. For enynes having an –NTs tether, yields ranged from 0–99% (Scheme 1, **5a**–**5e**). Of these enynes, the phenyl-substituted alkyne gives **5a** in 99% yield, the methyl- and methyl ester-substituted alkynes give **5b** and **5c** in 71% and

64% yield, and the terminal alkyne gives **5d** in 34% yield. Unlike substituted enyne precursors, dimer **5da** was obtained in 35% yield when the unsubstituted terminal alkyne underwent asymmetric PKR. For the TMS-substituted enyne only recovered starting material was observed after 18 h (**5e**). Additional methyl groups in the tether, likely due to the Thorpe-Ingold effect, accelerated the reaction to give product **5f** in 13 h compared to the 22 h required for complete conversion to product **5a**.[48] For the –NTs tethered substrates, high selectivities were observed for the terminal alkyne giving **5e** with an er of 99.8: 0.2, and the phenyl- methyl- and methyl ester-substituted alkynes giving **5a**, **5b,** and **5c** in 97:3 to 95:5 ers. An exception is the enyne having additional methyl groups in the tether giving **5f** in 83:17 er.

For ether tethered enynes, 63–90% yield was observed (**7a**–**7e**). Of these enynes, the electron-withdrawing phenyl- and trifluoroaryl-substituted enynes give **7a** and **7d** in 84% and 90% yield. The electron-donating fluoro- and methoxy-aryl groups give 63% and 76% yields of **7c** and **7e** and for the methyl-substituted alkyne, **7b** was afforded in 66% yield along with significant quantities of **7bi**. For the selectivities of the ether-tethered substrates, with the exception of **7a**, the ers were constant having a range from 84:16 to 87:13. For the malonate tethered enynes, the phenyl and the methyl-substituted alkynes give **9a** and **9b** in 94% and 93% yield; having ers of 90:10 and 78:22, respectively. The terminal alkyne gives only the side-product **9cs**.

Conversely, the nature of the tether has the greatest influence on selectivity, with the highest % *ee* observed for precursors with –NTs tethers (90–99.6% *ee*), with the exception of *gem*-dimethyl product **5f**. Selectivity was more moderate for ether tethered enynes (69–89% *ee*), and low to moderate for the all-carbon tethered enynes (43–80% *ee*). The yield and selectivity patterns observed with these 2,2-disubstituted alkene enynes are similar to those observed previously for enynes with a mono-substituted alkene.[49]

For the –NTs tethered substrates, a range of selectivities were observed. To quantify the steric effect, we plotted Sterimol values (B_1, B_5, and L) for the lowest-energy conformers of the PKR products **5a**, **5b**, **5c,** and **5d** against their ln(*ee*). The PKR products were selected for Sterimol analysis due to their rigidity and structural similarity to the oxidative cyclization transition state – the enantiodetermining step of these PKRs. Sterimol B_1 (Å) values, with the primary axis along the H_b–C bond, show a strong linear relationship ($R^2 = 0.96$) with PKR ln(*ee*), with smaller B_1 values giving higher % *ee* (Figure 7). Sterimol B_5 gives a low correlation ($R^2 = 0.53$) and Sterimol L gives a moderate correlation ($R^2 = 0.83$) with ln(*ee*) (see Figures S43–S44 in SI). Using (*R*)-BINAP as a chiral ligand, our experimental % *ees* show a linear free energy relationship (R^2=0.99) with the computed $\Delta\Delta G^{\ddagger}$ for the oxidative cyclization step reported by Baik and Evans using (*S*)-Xyl-SEGPHOS as the chiral ligand (see Figure S41 in SI).[26]

Scheme 1. Current scope of the asymmetric Pauson-Khand reactions

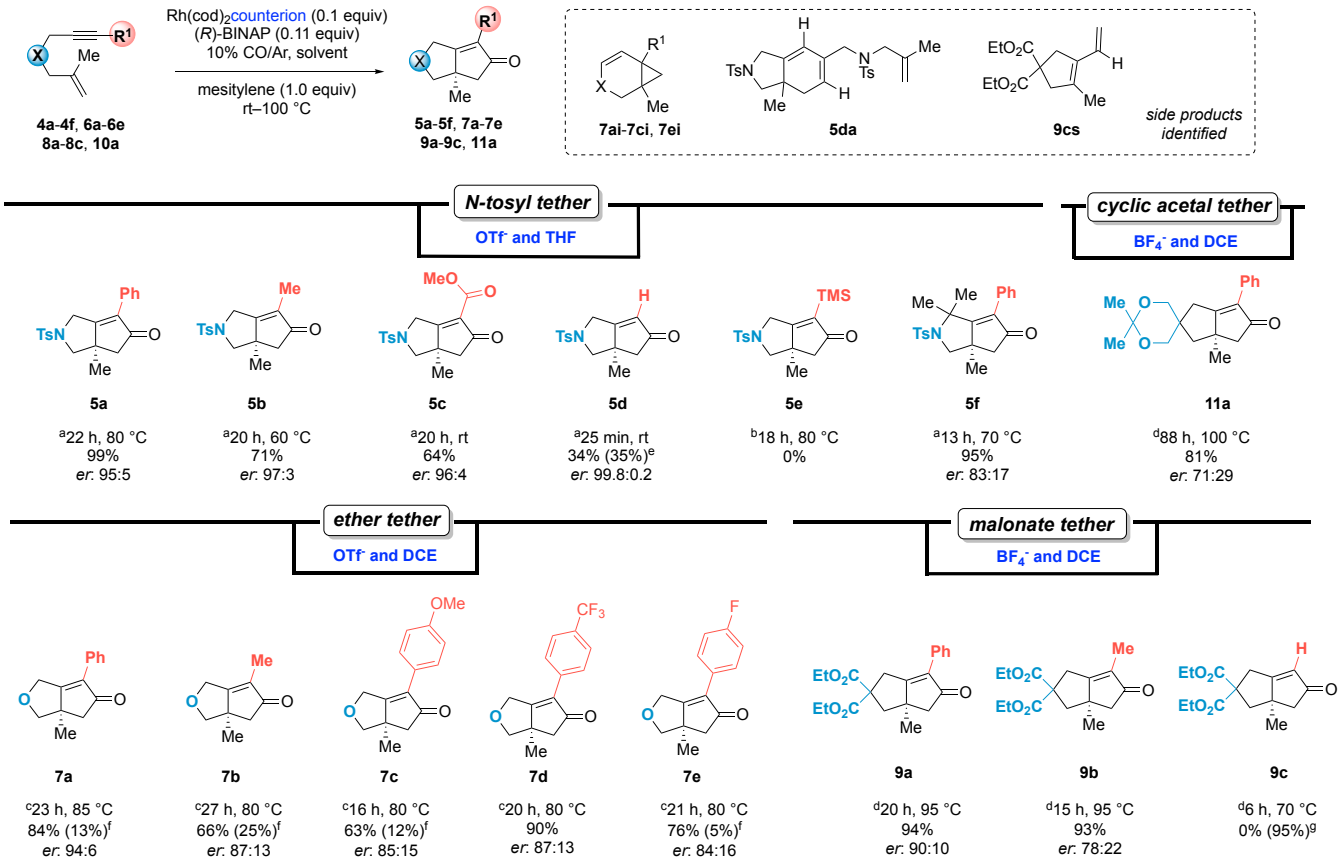

[a]$Rh(cod)_2OTf$ (0.1 equiv) in THF (0.05 M); [b]$Rh(cod)_2BF_4$ (0.1 equiv) in THF (0.05 M); [c]$Rh(cod)_2OTf$ (0.1 equiv) in DCE (0.05 M); [d] $Rh(cod)_2BF_4$ (0.1 equiv) in DCE (0.05 M); [e]yield of the [2+2+2] cycloaddition side-product **5da**; [f]yields of the cycloisomerized side products;[g]yield of the side product **9cs**

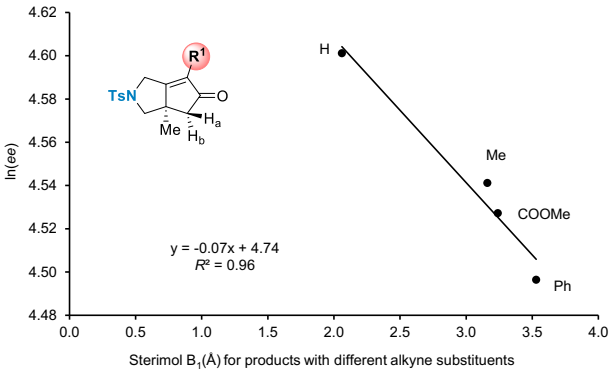

Figure 7. Correlation of ln(*ee*) with the calculated Sterimol B_1 (Å) for products **5a–5d.**

For the ether tether, electronic effects of the phenyl substituted alkyne showed product **7a** having the highest % *ee*, while **7c**, **7d**, and **7e** containing either electron-donating or electron-withdrawing groups formed with lower selectivity. The mass balance for these substates was high, with varying quantities of cycloisomerized products (5–13%) observed. We attribute the formation of this side-product mainly to the DCE solvent and counterion, as discussed above. In this case, malonate-tethered enynes afforded products **9a** and **9b** in excellent yield (94% and 93%, respectively). The cyclic acetal substituted product **11a** was formed 81% yield, albeit in only moderate selectivity (43% *ee*). However, the unsubstituted terminal alkyne afforded only side product **9cs**; the desired product **9c** was not observed. We also found that carbon-tethered enynes required elevated temperatures (95–100 °C), relative to the heteroatom-tethers (rt–85 °C), likely due to their lower reactivity, which has been explained by a distortion-interaction analysis involving the relatively planar geometry of the outer five-membered ring in the PKR oxidative cyclization step.[26]

To quantify the effect of the alkynyl group on yield, we computed IR C≡C bond wavenumber for each enyne precursor.[50] Precursors that underwent PKR in moderate to high yields consistently show an alkyne IR wavenumber exceeding 2250 cm^{-1}. Conversely, for precursors with an alkyne wavenumber ≤ 2203, low yields or no reaction were observed (see Table S8 in SI).

CONCLUSION

We have achieved an asymmetric Rh(I)-catalyzed PKR for 1,6-enynes having 2,2-disubstituted alkenes, allowing access to thirteen new chiral non-racemic bicyclo[3.3.0]octenone products having a quaternary carbon at the ring fusion. In the process, two descriptors for the chiral bisphosphine ligand have been identified that are strongly correlated with PKR ln(*ee*). In addition, catalysts that are predicted to have the weakest ion-pairing, as determined by their counterion, provided the fastest reactions and the highest yields for heteroatom-tethered enynes. Further, the dipole moment (D) and Abraham's hydrogen bond basicity (β) of the solvent show a strong correlation with PKR ln(*ee*). Finally, calculated Sterimol B_1 values correlate with ln(*ee*) and IR C≡C bond wavenumber correlates with reaction efficiency for variously substituted enyne PKR precursors. These findings are informing our high-throughput experimentation (HTE) studies to be performed in collaboration with Merck, Inc. In turn, we expect that the combination of these initial studies with statistical analysis of HTE data will facilitate the development of a predictive model for a catalyst-controlled Rh(I)-catalyzed asymmetric PKR of enynes. Such a framework will enable the rational selection of appropriate chiral catalysts and reaction conditions for a particular enyne in order to give the PKR product in high yield and high enantioselectivity.

ASSOCIATED CONTENT

Supporting Information.
The supporting information is available free of charge via the Internet at http://pubs.acs.org
Experimental details, spectral data of the new compounds, and HPLC analytical data (PDF)

Crystallographic data of (*R*)-5ax (cif)

Crystallographic data of 5ai (cif)

AUTHOR INFORMATION

Corresponding Authors

Peng Liu–Department of Chemistry, University of Pittsburgh, Pittsburgh, Pennsylvania 15260, United States; Department of Chemical and Petroleum Engineering, University of Pittsburgh, Pittsburgh, Pennsylvania 15261, United States; orcid.org/0000-0002-8188-632X; Email:pengliu@pitt.edu

Kay M. Brummond–Department of Chemistry, University of Pittsburgh, Pittsburgh, Pennsylvania 15260, United States; orcid.org/0000-0003-3595-6806; Email:kbrummon@pitt.edu

Authors

Yifan Qi–Department of Chemistry, University of Pittsburgh, Pittsburgh, Pennsylvania 15260, United States

Luke T. Jesikiewicz–Department of Chemistry, University of Pittsburgh, Pittsburgh, Pennsylvania 15260, United State

Grace E. Scofield– Department of Chemistry, University of Pittsburgh, Pittsburgh, Pennsylvania 15260, United State

Author Contributions

The manuscript was written through contributions of all authors. / All authors have given approval to the final version of the manuscript. /

Funding Sources

NIGMS (R35 GM128779)

Notes

The authors declare no competing financial interest.

ACKNOWLEDGMENT

We thank the NIGMS (R35 GM128779) and the University of Pittsburgh for financial support. DFT calculations were carried out at the

University of Pittsburgh Center for Research Computing and the Advanced Cyberinfrastructure Coordination Ecosystem: Services & Support (ACCESS) program, supported by NSF award numbers OAC-2117681, OAC-1928147, and OAC-1928224. The authors thank Dr. Steve Geib (University of Pittsburgh) for the data collection on X-ray crystallography and refinement.

REFERENCES

(1) Yang, Z. Navigating the Pauson–Khand Reaction in Total Syntheses of Complex Natural Products. *Acc. Chem. Res.* **2021**, *54*, 556–568.

(2) Heravi, M. M.; Mohammadi, L. Application of Pauson–Khand Reaction in the Total Synthesis of Terpenes. *RSC Adv.* **2021**, *11*, 38325–38373.

(3) Chen, S.; Jiang, C.; Zheng, N.; Yang, Z.; Shi, L. Evolution of Pauson-Khand Reaction: Strategic Applications in Total Syntheses of Architecturally Complex Natural Products (2016–2020). *Catalysts* **2020**, *10*, 1199.

(4) Ma, K.; Martin, B. S.; Yin, X.; Dai, M. Natural Product Syntheses *via* Carbonylative Cyclizations. *Nat. Prod. Rep.* **2019**, *36*, 174–219.

(5) Exon, C.; Magnus, P. Stereoselectivity of Intramolecular Dicobalt Octacarbonyl Alkene-Alkyne Cyclizations: Short Synthesis of *dl*-Coriolin. *J. Am. Chem. Soc.* **1983**, *105*, 2477–2478

(6) Magnus, P.; Exon, C.; Albaugh-Robertson, P. Dicobaltoctacarbonyl-Alkyne Complexes as Intermediates in the Synthesis of Bicyclo[3.3.0]Octenones for the Synthesis of Coriolin and Hirsutic Acid. *Tetrahedron* **1985**, *41*, 5861–5869

(7) Clark, J. S.; Xu, C. Total Synthesis of (−)-Nakadomarin A. *Angew. Chem. Int. Ed.* **2016**, *55*, 4332–4335.

(8) Huang, Z.; Huang, J.; Qu, Y.; Zhang, W.; Gong, J.; Yang, Z. Total Syntheses of Crinipellins Enabled by Cobalt-Mediated and Palladium-Catalyzed Intramolecular Pauson–Khand Reactions. *Angew. Chem.* **2018**, *130*, 8880–8884.

(9) Jiang, B.; Li, M.-M.; Xing, P.; Huang, Z.-G. A Concise Formal Synthesis of (−)-Hamigeran B. *Org. Lett.* **2013**, *15*, 871–873.

(10) Moriarty, R. M.; Rani, N.; Enache, L. A.; Rao, M. S.; Batra, H.; Guo, L.; Penmasta, R. A.; Staszewski, J. P.; Tuladhar, S. M.; Prakash, O.; Crich, D.; Hirtopeanu, A.; Gilardi, R. The Intramolecular Asymmetric Pauson–Khand Cyclization as a Novel and General Stereoselective Route to Benzindene Prostacyclins: Synthesis of UT-15 (Treprostinil). *J. Org. Chem.* **2004**, *69*, 1890–1902

(11) López-Pérez, B.; Maestro, M. A.; Mouriño, A. Total Synthesis of 1α,25-Dihydroxyvitamin D_3 (Calcitriol) through a Si-Assisted Allylic Substitution. *Chem. Commun.* **2017**, *53*, 8144–8147.

(12) Burrows, L. C.; Jesikiewicz, L. T.; Lu, G.; Geib, S. J.; Liu, P.; Brummond, K. M. Computationally Guided Catalyst Design in the Type I Dynamic Kinetic Asymmetric Pauson–Khand Reaction of Allenyl Acetates. *J. Am. Chem. Soc.* **2017**, *139*, 15022–15032.

(13) Kim, D. E.; Choi, C.; Kim, I. S.; Jeulin, S.; Ratovelomanana-Vidal, V.; Genêt, J. P.; Jeong, N. The Electronic Effect of Ligands on Stereoselectivity in the Rhodium(I)-Catalyzed Asymmetric Pauson-Khand-Type Reaction under a Carbon Monoxide Atmosphere. *Synthesis* **2007**, 4053–4059.

(14) Lu, Z.-L.; Neumann, E.; Pfaltz, A. Asymmetric Catalytic Intramolecular Pauson–Khand Reactions with Ir(phox) Catalysts. *Eur. J. Org. Chem.* **2007**, *2007*, 4189–4192.

(15) Lu, Z.; Li, T.; Mudshinge, S. R.; Xu, B.; Hammond, G. B. Optimization of Catalysts and Conditions in Gold(I) Catalysis—Counterion and Additive Effects. *Chem. Rev.* **2021**, *121*, 8452–8477.

(16) Burrows, L. C.; Jesikiewicz, L. T.; Liu, P.; Brummond, K. M. Mechanism and Origins of Enantioselectivity in the Rh(I)-Catalyzed Pauson–Khand Reaction: Comparison of Bidentate and Monodentate Chiral Ligands. *ACS Catal.* **2021**, *11*, 323–336.

(17) Choi, Y. H.; Kwak, J.; Jeong, N. Solvent Effects on the Asymmetric Pauson–Khand-Type Reaction by Rhodium. *Tetrahedron Lett.* **2009**, *50*, 6068–6071.

(18) Shibata, T.; Toshida, N.; Takagi, K. Rhodium Complex-Catalyzed Pauson–Khand-Type Reaction with Aldehydes as a CO Source. *J. Org. Chem.* **2002**, *67*, 7446–7450.

(19) Kwong, F. Y.; Lee, H. W.; Qiu, L.; Lam, W. H.; Li, Y.-M.; Kwong, H. L.; Chan, A. S. C. Rhodium-BisbenzodioxanPhoS Complex-Catalyzed Homogeneous Enantioselective Pauson–Khand-Type Cyclization in Alcoholic Solvents. *Adv. Synth. Catal.* **2005**, *347*, 1750–1754.

(20) Kwong, F. Y.; Li, Y. M.; Lam, W. H.; Qiu, L.; Lee, H. W.; Yeung, C. H.; Chan, K. S.; Chan, A. S. C. Rhodium-Catalyzed Asymmetric Aqueous Pauson–Khand-Type Reaction. *Chem. Eur. J.* **2005**, *11*, 3872–3880.

(21) Ikeda, K.; Morimoto, T.; Kakiuchi, K. Utilization of Aldoses as a Carbonyl Source in Cyclocarbonylation of Enynes. *J. Org. Chem.* **2010**, *75*, 6279–6282.

(22) Shibata, T.; Takagi, K. Iridium–Chiral Diphosphine Complex Catalyzed Highly Enantioselective Pauson-Khand-Type Reaction. *J. Am. Chem. Soc.* **2000**, *122*, 9852–9853.

(23) Shibata, T.; Toshida, N.; Yamasaki, M.; Maekawa, S.; Takagi, K. Iridium-Catalyzed Enantioselective Pauson–Khand-Type Reaction of 1,6-Enynes. *Tetrahedron* **2005**, *61*, 9974–9979.

(24) Kwong, F. Y.; Lee, H. W.; Lam, W. H.; Qiu, L.; Chan, A. S. C. Iridium-Catalyzed Cascade Decarbonylation/Highly Enantioselective Pauson–Khand-Type Cyclization Reactions. *Tetrahedron: Asymmetry* **2006**, *17*, 1238–1252.

(25) Fuji, K.; Morimoto, T.; Tsutsumi, K.; Kakiuchi, K. Catalytic Asymmetric Pauson–Khand-Type Reactions of Enynes with Formaldehyde in Aqueous Media. *Tetrahedron Lett.* **2004**, *45*, 9163–9166.

(26) Ylagan, R. M. P.; Lee, E. J.; Negru, D. E.; Ricci, P.; Park, B.; Ryu, H.; Baik, M.; Evans, P. A. Enantioselective Rhodium-Catalyzed Pauson–Khand Reactions of 1,6-Chloroenynes with 1,1-Disubstituted Olefins. *Angew. Chem. Int. Ed.* **2023**, *62*, e202300211

(27) Wu, G.; Wu, J.-R.; Huang, Y.; Yang, Y.-W. Enantioselective Synthesis of Quaternary Carbon Stereocenters by Asymmetric Allylic Alkylation: A Review. *Chem. Asian J.* **2021**, *16*, 1864–1877.

(28) Ling, T.; Rivas, F. All-Carbon Quaternary Centers in Natural Products and Medicinal Chemistry: Recent Advances. *Tetrahedron* **2016**, *72*, 6729–6777.

(29) Li, C.; Ragab, S. S.; Liu, G.; Tang, W. Enantioselective Formation of Quaternary Carbon Stereocenters in Natural Product Synthesis: A Recent Update. *Nat. Prod. Rep.* **2020**, *37*, 276–292.

(30) Kim, S. Y.; Chung, Y. K. Rhodium(I)-Catalyzed Cycloisomerization of 1,6-Enynes to Bicyclo[4.1.0]heptenes. *J. Org. Chem.* **2010**, *75*, 1281–1284.

(31) Ota, K.; Lee, S. I.; Tang, J.-M.; Takachi, M.; Nakai, H.; Morimoto, T.; Sakurai, H.; Kataoka, K.; Chatani, N. Rh(II)-Catalyzed Skeletal Reorganization of 1,6- and 1,7-Enynes through Electrophilic Activation of Alkynes. *J. Am. Chem. Soc.* **2009**, *131*, 15203–15211.

(32) Shintani, R.; Nakatsu, H.; Takatsu, K.; Hayashi, T. Rhodium-Catalyzed Asymmetric [5+2] Cycloaddition of Alkyne–Vinylcyclopropanes. *Chem. Eur. J.* **2009**, *15*, 8692–8694.

(33) Shibata, T.; Kobayashi, Y.; Maekawa, S.; Toshida, N.; Takagi, K. Iridium-Catalyzed Enantioselective Cycloisomerization of Nitrogen-Bridged 1,6-Enynes to 3-Azabicylo[4.1.0]heptenes. *Tetrahedron* **2005**, *61*, 9018–9024.

(34) Fan, B.-M.; Xie, J.-H.; Li, S.; Tu, Y.-Q.; Zhou, Q.-L. Rhodium-Catalyzed Asymmetric Pauson–Khand Reaction Using Monophosphoramidite Ligand SIPHOS. *Adv. Synth. Catal.* **2005**, *347*, 759–762.

(35) Kobayashi, T.; Koga, Y.; Narasaka, K. The Rhodium-Catalyzed Pauson–Khand Reaction. *J. Organomet. Chem.* **2001**, *624*, 73–87.

(36) Jeong, N.; Sung, B. K.; Choi, Y. K. Rhodium(I)-Catalyzed Asymmetric Intramolecular Pauson–Khand-Type Reaction. *J. Am. Chem. Soc.* **2000**, *122*, 6771–6772.

(37) Dotson, J. J.; van Dijk, L.; Timmerman, J. C.; Grosslight, S.; Walroth, R. C.; Gosselin, F.; Püntener, K.; Mack, K. A.; Sigman, M. S. Data-Driven Multi-Objective Optimization Tactics for Catalytic Asymmetric Reactions Using Bisphosphine Ligands. *J. Am. Chem. Soc.* **2023**, *145*, 110–121.

(38) Kim, D. E.; Choi, C.; Kim, I. S.; Jeulin, S.; Ratovelomanana-Vidal, V.; Genêt, J.-P.; Jeong, N. Electronic and Steric Effects of Atropisomeric Ligands SYNPHOS® and DIFLUORPHOS® *vs.* BINAPs in Rh(I)-Catalyzed Asymmetric Pauson–Khand Reaction. *Adv. Syn. Catal.* **2007**, *349*, 1999–2006.

(39) DFT calculations were performed at the M06/SDD-6-311+G(d,p)/SMD(DCE)//B3LYP-D3/LANL2DZ-6-31G(d) level of theory. See the Supporting Information (SI) for computational details.

(40) Substrate distortion energy, $\Delta E_{\text{dist-sub}}$, was calculated from the energy difference of the geometry of the enyne substrate in the oxidative cyclization transition state with respect to that in the enyne-Rh complexes (**6a-Rh-L1** and **6a-Rh-L3**).

(41) Kamlet, M. J.; Gal, J. F.; Maria, P. C.; Taft, R. W. Linear Solvation Energy Relationships. Part 32. A Coordinate Covalency Parameter, ξ, which, in Combination with the Hydrogen Bond Acceptor Basicity Parameter, β, Permits Correlation of many Properties of Neutral Oxygen and Nitrogen Bases (Including Aqueous pK_a). *J. Chem. Soc., Perkin Trans. 2* **1985**, 1583–1589.

(42) Dyson, P. J.; Jessop, P. G. Solvent Effects in Catalysis: Rational Improvements of Catalysts via Manipulation of Solvent Interactions. *Catal. Sci. Technol.* **2016**, 6, 3302–3316.

(43) Abraham, M. H.; Grellier, P. L.; Kamlet, M. J.; Doherty, R. M.; Taft, R. W.; Abboud, J.-L. M. The Use of Scales of Hydrogen-Bond Acidity and Basicity in Organic Chemistry. *Rev. Port. Quím* **1989**, *31*, 85–92

(44) Yang, P.; Zhang, Y.; Chen, M.; Zhao, Q.; Ren, Z.-H.; Guan, Z.-H. Rhodium-Catalyzed Enantioselective and Desymmetrizative Pauson–Khand Reaction: Access to Tricyclo[6.2.1.$0^{4,11}$]undecenes. *Org. Lett.* **2021**, *23*, 9241–9245.

(45) Furusawa, T.; Morimoto, T.; Ikeda, K.; Tanimoto, H.; Nishiyama, Y.; Kakiuchi, K.; Jeong, N. Asymmetric Pauson–Khand-Type Reactions of 1,6-Enynes Using Formaldehyde as a Carbonyl Source by Cooperative Dual Rhodium Catalysis. *Tetrahedron* **2015**, *71*, 875–881.

(46) Schmid, T. M.; Consiglio, G. Mechanistic and Stereochemical Aspects of the Asymmetric Cyclocarbonylation of 1,6-Enynes with Rhodium Catalysts. *Chem. Commun.* **2004**, 2318–2319.

(47) Soriano, E.; Ballesteros, P.; Marco-Contelles, J. A Theoretical Investigation on the Mechanism of the $PtCl_2$-Mediated Cycloisomerization of Heteroatom-Tethered 1,6-Enynes. *J. Org. Chem.* **2004**, *69*, 8018–8023.

(48) Inagaki, F.; Mukai, C. Rhodium(I)-Catalyzed Intramolecular Pauson–Khand-Type [2 + 2 + 1] Cycloaddition of Allenenes. *Org. Lett.* **2006**, *8*, 1217–1220.

(49) Kim, D. E.; Ratovelomanana-Vidal, V.; Jeong, N. 2,2'-Bis[bis(3,5-*tert*-butyl-4-methoxyphenyl)phosphino]-6,6'-dimethoxy-1,1'-biphenyl in Intramolecular Rhodium(I)-Catalyzed Asymmetric Pauson-Khand-Type Reactions. *Adv. Synth. Catal.* **2010**, *352*, 2032–2040

(50) Milo, A.; Bess, E. N.; Sigman, M. S. Interrogating Selectivity in Catalysis Using Molecular Vibrations. *Nature*. **2014**, *507*, 210–214.

Insert Table of Contents artwork here